Shear strength and stress distribution in wet granular media

Vincent Richefeu*, Farhang Radjaï† and Moulay Saïd El Youssoufi†

*Laboratoire 3S-R, Domaine Universitaire, B.P. 53, 38041 Grenoble Cedex 9, France
†LMGC - UMR CNRS 5508, Université Montpellier 2, C.C. 048, 34095 Montpellier Cedex 5, France

Abstract. We investigate the shear strength and stress distribution properties of wet granular media in the pendular state where the liquid is mainly in the form of capillary bonds between particles. This work is based on a 3D discrete-element approach (molecular dynamics) with spherical particles enriched by a capillary force law. We show that the capillary force can be expressed as an explicit function of the gap and volume of the liquid bridge. The length scales involved in this expression are analyzed by comparing with direct integration of the Laplace-Young equation. In the simulations, we consider a maximum number density of liquid bonds in the bulk in agreement with equilibrium of each liquid bridge. This liquid bond number is a decisive parameter for the overall cohesion of wet granular materials. It is shown that the shear strength can be expressed as a function of liquid bond characteristics. The expression proposed initially by Rumpf is thus generalized to account for size polydispersity. We show that this expression is in good agreement with our experimental data that will be briefly described. At low confining stress, the tensile action of capillary bonds induces a self-stressed particle network organized in a bi-percolating structure of positive and negative particle pressures. Various statistical descriptors of the microstructure and bond force network are used to characterize this partition. Two basic properties emerge: (i) The highest particle pressure is located in the bulk of each phase (positive and negative particle pressures); (ii) The lowest pressure level occurs at the interface between the two phases, involving also the largest connectivity of the particles via tensile and compressive bonds.

Keywords: capillary cohesion, discrete element approach, shear strength, self-stresses
PACS: 45.70.-n, 81.05.Rm, 83.80.Fg

INTRODUCTION

Cohesive granular media are of particular interest to the processing (compaction, granulation...) of fine powders or geomaterials. Although cohesive materials present strong similarities with dry granular media due to their common granular microstructure, the presence of cohesion induces new mechanisms such as particle aggregation affect the static and dynamic properties of the material.

In this paper, we use 3D molecular dynamics method in which capillary attraction between spherical particles is implemented as a force law expressing the capillary force as a function of the distance, water volume, and particle diameters. We first describe our model of capillary cohesion. The shear strength at low confinement pressures is then analysed by means of experimental and numerical direct shear tests. We show that the shear strength can be expressed as a function of liquid bond characteristics. In the last section, we introduce particle stresses and we analyze their distribution to characterize the organization of particle pressures which take positive or negative values according to their positions in the network of self-equilibrated bond forces. We will see that this organization involves a genuin partition of the particles in two phases of negative and positive pressures.

MODEL DESCRIPTION

We used the MD method with spherical particles and a capillary force law. The total normal force f_n at each contact is the sum of a repulsive force f_n^r and an attractive capillary force f_n^c. The latter is a function of the liquid bond parameters, namely the gap δ_n, the liquid bond volume V_b, the liquid surface tension γ_s, and the particle-liquid-gas contact angle θ; see inset in Fig. 1. The capillary force can be calculated by integrating the Laplace-Young equation [1, 2, 3]. However, for efficient MD simulations, we need an explicit expression of f_n^c as a function of the liquid bond parameters.

We used an analytical form for the capillary force which is well fitted by the data from direct integration of the Laplace-Young equation both for polydisperse particles [4]. At leading order, the capillary force f_0 at contact, i.e. for $\delta_n \leq 0$, is

$$f_0 = -\kappa\, R, \tag{1}$$

where R is a length depending on the particle radii R_i and R_j and κ is given by [5, 6, 7]

$$\kappa = 2\pi\gamma_s \cos\theta. \tag{2}$$

The adhesion force f_0 at contact (independent of the bond liquid volume V_b) is the highest value of the capillary force. The latter declines as the gap δ_n increases. The capillary bridge is stable as long as $\delta_n < \delta_n^{max}$, where

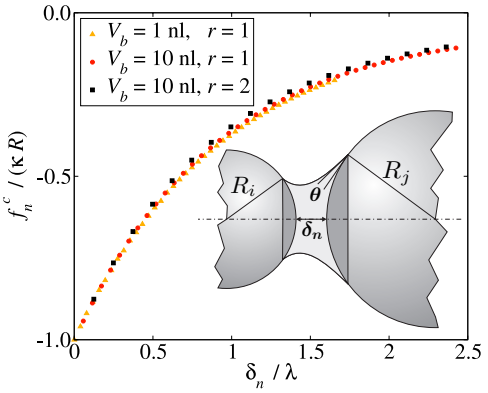

FIGURE 1. Scaled plot of the capillary force as a function of the gap between two particles for different values of the local liquid volume V_b and size ratio r according to the model proposed in this paper. Inset: Geometry of a capillary bridge.

δ_n^{max} is the debonding distance given by [8]

$$\delta_n^{max} = \left(1 + \frac{\theta}{2}\right) V_b^{1/3}. \tag{3}$$

Between these two limits, the capillary force falls off exponentially with δ_n:

$$f_n^c = f_0 e^{-\delta_n/\lambda}, \tag{4}$$

where λ is a length scale which should be a function of V_b and the particle radii. The asymmetry due to unequal particle sizes is taken into account through a function of the ratio between particle radii. We set

$$r = \max(R_i/R_j \; ; \; R_j/R_i). \tag{5}$$

Dimensionally, a plausible expression of λ is

$$\lambda = c\, h(r) \left(\frac{V_b}{R'}\right)^{1/2}, \tag{6}$$

where c is a constant and h is a function only of r. When introduced in Equations (6) and (4), this form yields a nice fit for the capillary force obtained from direct integration of the Laplace-Young equation by setting $R' = 2R_iR_j/(R_i+R_j)$, $h(r) = r^{-1/2}$ and $c \simeq 0.9$.

Figure 1 shows the plots of Eq. 4 for three different values of the liquid volume V_b and size ratio r together with the corresponding data from direct integration. The forces are normalized by κR and the lengths by λ. The data collapse on the same plot, indicating again that the force κR and the expression of λ in Eq. (6) characterize correctly the behavior of the capillary bridge. Finally, the capillary force can be expressed in the following form:

$$f_n^c = \begin{cases} -\kappa\, R & \text{for} \quad \delta_n < 0 \\ -\kappa\, R\, e^{-\delta_n/\lambda} & \text{for} \quad 0 \le \delta_n \le \delta_n^{max} \\ 0 & \text{for} \quad \delta_n > \delta_n^{max} \end{cases} . \tag{7}$$

In the simulations, the total liquid volume is distributed among all eligible particle pairs (the pairs with a gap below the debonding distance, including the contact points) in proportion to the reduced diameter of each pair. We also assume that the particles are perfectly wettable, i.e. $\theta = 0$. The choice of the water volume has no influence on the value of the largest capillary force in the pendular state [9]. For our simulations, we chose a gravimetric water content lower than 0.05 so that the material is in the pendular state. The coefficient of friction is $\mu = 0.4$ in all simulations.

SHEAR STRENGTH

For the shear strength analysis, we performed both experimental and numerical direct shear tests. The experiments were carried out with glass beads and sand by means of a setup especially designed for weak confining stresses (below 1 kPa) in order to enhance the capillary effects [9]. Both experimental and numerical results were analyzed in the Mohr-Coulomb space. We found that the internal angle of friction was not sensitive to water content w and the Coulomb cohesion increased in a nonlinear fashion with w to reach a limit value at a well-defined level c_m of cohesion independent of water content. A similar behavior was observed in numerical simulations. The cohesion c_m was found to be quite close between the experiments and numerics for the samples of the same particle size distribution ($c_m = 120$ Pa in numerics vs. $c_m = 150$ Pa in experiments).

Let us consider the general expression of the stress tensor σ in a granular material. This is an average quantity with an expression involving contact forces f^k and branch vectors ℓ^k :

$$\sigma_{ij} = \frac{1}{V} \sum_{k \in V} f_i^k \ell_j^k \,, \tag{8}$$

where i and j refer to the components and V is the control volume. The set of contact points in a wet material is extended to include gap capillary bridges. From Eq. 8, we get the following expression for the stress p in the direction of extension:

$$p = n_w \langle f_n \; \ell \rangle \,, \tag{9}$$

where n_w is the number of bonds per unit volume, f_n is the normal force and ℓ is the distance between particle centers. The symbol $\langle \cdots \rangle$ designs averaging over all bonds in the control volume V.

Our simulations show that the fraction of liquid bonds in the range $\delta_n > 0$ (gap liquid bridges) is always below 15%. This means that most tensile stresses occur at contact bonds and, as a result, the capillary failure threshold f_0 is far more important for the failure of a wet material

than the de-bonding distance δ_n^{max}. We may thus get a good estimation of the tensile strength for a wet particle assembly by replacing f_n in Eq. 9 by the capillary force threshold f_0 and by assuming, for simplicity, that the material is isotropic (a correction due to anisotropy can then easily be made):

$$\sigma^{th} = \frac{n_w}{D}\langle f_0\ \ell\rangle, \tag{10}$$

where D is space dimension. The bond density n_w is equal to half the average number of bonds per particle divided by the free volume, i.e. the mean volume of a Voronoi cell surrounding the particle. The latter is simply the average particle volume $(1/6)\pi\langle d^3\rangle$ divided by the solid fraction ϕ. Introducing these expressions in Eq. 10 and using Eq. 2, we get

$$\sigma^{th} = \frac{3\kappa\ \phi\ z}{\pi D}\frac{\langle (R_1+R_2)\sqrt{R_1R_2})\rangle}{\langle d^3\rangle} = \frac{3}{2\pi D}s\ \frac{\kappa\ \phi\ z}{\langle d\rangle}, \tag{11}$$

where z is the average number of bonds per particle, and we have

$$s = \frac{\langle d^{1/2}\rangle\langle d\rangle\langle d^{3/2}\rangle}{\langle d^3\rangle}. \tag{12}$$

In derivation of the expression of s, it is assumed that the particle radii R_1 and R_2 are not correlated. It is easy to see that for a uniform size distribution, s varies from $8/15$ to 1 as the smallest particle size increases from 0 to the mean particle size. Eq. 11 is similar to the expression proposed first by Rumpf for monodisperse materials without the s prefactor, and recently derived from the stress tensor by Gröger et al. [10]. Our equation 11 accounts for polydispersity and the correlation between the capillary force threshold f_0 and the particle size d.

As in experiments, our simulations show that the internal angle of friction μ is practically independent of water content. Hence, from Eq. 11 we get the following expression for the Coulomb cohesion $c^{th} = \mu\sigma^{th}$:

$$c^{th} = \frac{3}{2\pi D}\mu\ \kappa\ s\ \frac{\phi\ z}{\langle d\rangle}. \tag{13}$$

We found that the Coulomb cohesion calculated from the simulations of polydisperse materials is in good agreement with the theoretical estimate by Eq. 13. It is worth noting that important discrepancy would arise if the polydispersity were ignored; i.e. with $s = 1$. On the other hand, Eq. 13 suggests that the Coulomb cohesion increases nonlinearly with water content as the average bond connectivity z (not shown in this paper; for details see [9]). The simulations are in good agreement with this prediction.

It is important to note that the water content does not enter the above expression of c^{th}. The only parameter related to water is κ. This suggests that the water content manifests itself mainly through the average number of bonds per particle z. In particular, the cohesion c_m at saturation corresponds to the saturation of z as the water content w is increased. In fact, when a certain amount of water is homogeneously distributed in the whole sample within the de-bonding distance, one finds that z increases with w and saturates beyond a certain amount of water.

BI-PERCOLATING STRUCTURE OF SELF-STRESSES

In an unconfined assembly of dry rigid particles, no self-stresses occur and the forces vanish at all contacts. However, we have seen that the presence of liquid bonds in a wet granular material induces tensile and compressive forces although the average force is zero. In other words, the grains keep together to form a self-sustained structure in the absence of confining stresses. In general, various loading histories such as consolidation or differential particle swelling can induce self-stresses in a cohesive packing [11, 12]. In our system, the self-stresses appear during relaxation. This is obviously a consequence of the tensile action of capillary bonds bridging the gaps between neighboring particles within the debonding distance. We focus here on the structure of self-stresses induced by capillary bonds.

For a local description of self-stresses we need to characterize the stress transmission at the particle scale as the smallest scale at which the force balance condition is defined for rigid particles. Although the stress tensor is by definition a macroscopic quantity, it can be shown that an equivalent quantity σ_i, called 'particle stress', can be defined for each particle i of a granular packing in static equilibrium [13, 14]:

$$(\sigma_i)_{\alpha\beta} = \frac{1}{V_i}\sum_{j\neq i} f_\alpha^{ij} r_\beta^{ij}, \tag{14}$$

where r_{ij} is the position of the contact-point of the force f_{ij} of particle j on particle i, and α and β design the Cartesian components. V_i is the free volume of particle i, the sum of the particle volume and a fraction of the pore space $V_i = \pi d_i^3/6\nu$, where d_i is the particle diameter, and ν is the solid fraction of the packing. The sum of particle stresses σ_i weighted by the corresponding relative free volumes V_i/V tends to the Cauchy stress tensor as the number of particles in a control volume V increases.

From the particle stresses we get the particle pressures $p_i = \frac{1}{3}\sum_{\alpha=1}^{3}(\sigma_i)_{\alpha\alpha}$. Each particle can take on positive or negative pressures according to the forces exerted by neighboring particles. The pdf of particle pressures is displayed in Fig. 2 for the unconfined sample. The pressures have been normalized by a reference pressure $p_0 = f_0/\langle d\rangle^2$. The distribution is symmetric around and

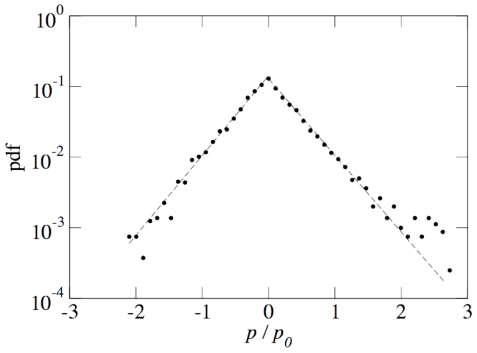

FIGURE 2. Probability density function of particle pressures normalized by the reference pressure p_0 (see text) in the unconfined wet packing.

peaked on zero pressure, and each part is well fit by an exponential form.

Zero particle pressure corresponds to a state where a particle is balanced under the combined action of tensile and compressive forces. Such particle states are not marginal here and they reflect a particular stress transmission in a wet packing. The positive and negative particle pressures may form separate phases mixing together at large scales or mix together at the particle scale. Fig. 3, displaying the packing where the positive and negative pressures are represented in different colors, credits rather the first scenario. We observe that the particles of either positive or negative pressure appear as two separate phases each percolating throughout the system. The morphology of each phase is approximately filamentary with variable thickness and a large interface between them. A detailed analysis of this structure shows that the particles at the interface between the two phases have a weak pressure and the largest negative or positive pressures are located at the heart of each phase [14].

CONCLUSION

In this paper, we presented an analytical expression of the capillary force as a function of geometrical and materials parameters of a liquid bridge, and it was shown that it provides excellent fit for the data from direct integration of Laplace-Young equations. By means of three-dimensional discrete element simulations including our capillary law, we analyzed shear strength and stress transmission in wet granular packings submitted to very low confinement pressures.

Starting with the expression of the stress tensor, we introduced a novel expression for the Coulomb cohesion as a function of material and structural parameters. This expression extends the classical model of Rumpf to polydisperse materials.

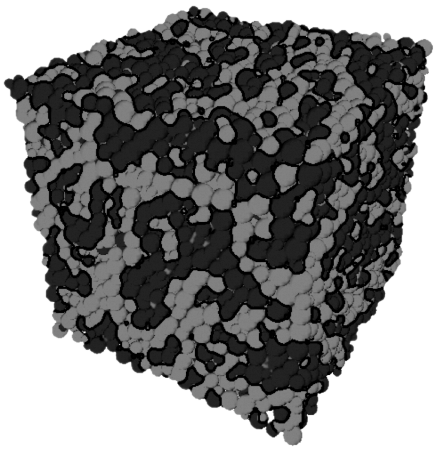

FIGURE 3. The unconfined wet packing with negative (white) and positive (black) particle pressures.

For wet granular media with a homogeneous distribution of liquid, we showed the nontrivial organization of particle pressures in the form of two separate percolating phases of tensile and compressive particle pressures with an interphase at zero pressure.

REFERENCES

1. M. A. Erle, D. C. Dyson, and N. R. Morrow, AIChE Journal **17**, 115 (1971)
2. T. Mikami, H. Kamiya, and M. Horio, Chemical Engineering Science **53**, 1927 (1998)
3. F. Soulié, F. Cherblanc, M. S. El Youssoufi, and C. Saix, Int. J. Numer. Analyt. Meth. Geomech. **30**, 213 (2006)
4. V. Richefeu, M. S. El Youssoufi, R. Peyroux and F. Radjaï, Int. J. Numer. Anal. Meth. Geomech. **32**(11), 1365 (2007)
5. C. Willett, M. Adams, S. Johnson, and J. Seville, Langmuir **16**, 9396 (2000)
6. L. Bocquet, E. Charlaix, F. Restagno, C. R. Physique 3, 207 (2002)
7. S. Herminghaus, Advances in Physics **54**, 221 (2005)
8. G. Lian, C. Thornton, and M. J. Adams, Chem. Eng. Sci. **53**, 3381 (2004)
9. V. Richefeu, M. S. El Youssoufi and F. Radjaï, Phys. Rev. E **73**, 051304 (2006)
10. T. Gröger, U. Tüzün, and D. Heyes, Powder Technology [133], 203 (2003)
11. F. Radjaï, I. Preechawuttipong, R. Peyroux, in Continuous and Discontinuous Modelling of Cohesive-Frictional Materials, edited by P. A. Vermeer, S. Diebels, W. Ehlers, H.J. Hermann, S. Luding, E. Ramm (Springer, Berlin, 2001) p. 149
12. M. S. El Youssoufi, J.-Y. Delenne, and F. Radjaï, Phys. Rev. E **71**, 051307 (2005).
13. L. Staron, F. Radjaï, and J.-P. Vilotte, Eur. Phys. J. E **18**, 311 (2005)
14. V. Richefeu, F. Radjaï and M. S. El Youssoufi, Eur. Phys. J. E **21**, 359-369 (2006)